Heat fluctuations and coherences in a quantum heat engine

Saar Rahav, Upendra Harbola, and Shaul Mukamel

Heat fluctuations and coherences in a quantum heat engine

Saar Rahav[1], Upendra Harbola[2], and Shaul Mukamel[3]

[1]Schulich Faculty of Chemistry, Israel Institute of Technology, Haifa 32000, Israel.
[2]Department of inorganic and physical chemistry,
Indian Institute of Science, Bangalore, 560012, India. and
[3]Department of chemistry, University of California, Irvine, USA.

Quantum coherence can affect the thermodynamics of small quantum systems. Coherences have been shown to affect the power generated by a quantum heat engine (QHE) which is coupled to two thermal photon reservoirs and to an additional cavity mode. We show that the fluctuations of the heat exchanged between the QHE and the reservoirs strongly depend on quantum coherence, especially when the engine operates as a refrigerator, i.e. heat current flows from the cold bath to the hot bath. Intriguingly, we find that the ratio of positive and negative (with respect to thermodynamic force) fluctuations in the heat current satisfies a universal coherence-independent fluctuation theorem (FT).

I. INTRODUCTION

Photovoltaic cells harness the solar energy to produce electric charge which is used to perform work [1, 2]. Current photo cell technology reaches efficiencies which are too small to allow solar energy to meet our day-to-day power needs [3]. Recent advances in the fabrication of quantum dots (QDs) have provided new approaches for enhancing photo cell efficiencies. [4–8].

Quantum effects such as coherence are particularly important in these small sized systems. In recent studies, Scully and coworkers [9, 10] have analyzed the working of a photovoltaic cell by modeling it as a collection of a finite set of electronic levels resonantly coupled to thermally populated field modes at different temperatures. A laser heat engine, or more generally a quantum heat engine (QHE), is a quantum system that converts incoherent phonon energy of thermal baths to coherent laser field. The working mechanisms of a photo cell and a QHE are very similar. Both, the photocell and the QHE, have been modeled using the same level scheme [9].

The thermodynamic properties of such QHEs were extensively studied [11–13] and found to satisfy the classical Carnot's Shockley-Queisser [14] bound on efficiency. Recently, it has been demonstrated that quantum effects can dramatically change the thermodynamics of QHEs. Examples include lasing without inversion [15], reduction of radiative recombination in photocells [10], extraction of work from a single thermal reservoir[16], and enhancement of the output power of a QHE [9].

The relative importance of fluctuations typically increases as the size of the system decreases, and a single realization of an experiment is no longer well approximated by the mean behavior. In this work we analyze quantum effects on the fluctuations in the output power of a QHE. There is a considerable interest in understanding fluctuations in far from equilibrium quantum systems [17, 18]. A good measure of these fluctuations is provided by their full counting statistics (FCS), namely the full probability distribution for the number of particles or energy exchanged during a given time interval. The FCS is commonly used to characterize electron transfer in nanojunctions [19, 20].

A family of relations collectively known as Fluctuation Theorems (FTs) were found to hold in systems arbitrarily far from equilibrium [21–24]. While the first FTs were derived for classical systems, FTs were shown to hold for quantum models [25–27]. The FTs appear as a constraint that the FCS generating function must satisfy.
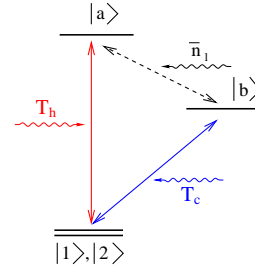

FIG. 1. (Color online) The level scheme of the QHE model. A pair of degenerate levels $|1\rangle, |2\rangle$ is resonantly coupled to two excited levels $|a\rangle$ and $|b\rangle$ by two thermally populated field modes with hot (T_h) and cold (T_c) temperatures. Levels $|a\rangle$ and $|b\rangle$ are coupled by a non thermal cavity mode. Emission of photons into this mode is interpreted as work.

Here we show that apart from enhancing the yield of the QHE [9], quantum effects also influence the full counting statistics of fluctuations significantly. We further show that a universal relation between the probability of positive and negative (with respect to thermodynamic force) fluctuations (FT) holds. Curiously, we find that, unlike fluctuations, the FT is universal and independent of quantum effects.

The QHE model is presented in the next section. The steady state properties of the model are studied in section III. In particular, the influence of quantum coherence on the QHE current is investigated. In section IV we examine how coherence affects the distribution of heat that the QHE exchanges with the hot reservoir. Results

are summarised in section V.

II. THE FOUR LEVEL QHE MODEL

We use the same QHE model as introduced by Scully [9]. A four level quantum system is coupled to two thermal reservoirs at temperatures T_h and $T_c < T_h$ (Fig. (1)), and to an additional cavity mode, which has a single mode. The work done by the machine enhances this mode coherently by stimulated emission.

The Hamiltonian for our four level quantum heat engine (QHE) is given by

$$\hat{H}_0 = \sum_{\nu=1,2,a,b} E_\nu \hat{B}_{\nu\nu} + \sum_k \epsilon_k \hat{a}_k^\dagger \hat{a}_k + \epsilon_l \hat{a}_l^\dagger \hat{a}_l, \quad (1)$$

where the terms correspond to the four level system, heat baths and the cavity mode, respectively. The coupling between various components is described by

$$\hat{H} = \sum_{k,i=1,2} g_{ik} \hat{a}_k \hat{B}_{ia}^\dagger + h.c. \quad (2)$$

Finally, the coupling of states $|a\rangle$ and $|b\rangle$ via the cavity mode is

$$\hat{V} = g(\hat{a}_l^\dagger \hat{B}_{ba} + \hat{B}_{ba}^\dagger \hat{a}_l), \quad (3)$$

where $\hat{B}_{\nu\nu'} = |\nu\rangle\langle\nu'|$ represents the excitation operator between states $|\nu\rangle$ and $|\nu'\rangle$, $\hat{a}^\dagger(\hat{a})$ denotes creation (annihilation) operators for harmonic modes in thermal baths and in the electromagnetic field. g (real number) is the coupling strength between the system and the radiation field.

One of the intriguing properties of the model is that second order coupling of the states $|1\rangle, |2\rangle$ to any of the high lying levels, which typically leads to rate equations for the populations, can induce coherence between the $|1\rangle, |2\rangle$ states. The dynamics of the QHE can be described by a Lindblad equation, $\frac{d}{dt}\rho = \mathcal{L}\rho$ [9] where the vector $\rho = \{\rho_{11}, \rho_{22}, \rho_{aa}, \rho_{bb}, \bar{\rho}_{12}\}$ contains the steady state populations and coherences. The Lindblad operator is

$$\mathcal{L} = \begin{pmatrix} g_{11} & 0 & \gamma_{1h}\tilde{n}_h & \gamma_{1c}\tilde{n}_c & -2g_{12} \\ 0 & g_{22} & \gamma_{2h}\tilde{n}_h & \gamma_{2c}\tilde{n}_c & -2g_{12} \\ \gamma_{1h}\bar{n}_h & \gamma_{2h}\bar{n}_h & g_{aa} & g^2\tilde{n}_l & 2\gamma_{12h}\bar{n}_h \\ \gamma_{1c}\bar{n}_c & \gamma_{2c}\bar{n}_c & g^2\tilde{n}_l & g_{\beta\beta} & 2\gamma_{12c}\bar{n}_c \\ -g_{12} & -g_{12} & \gamma_{12h}\tilde{n}_h & \gamma_{12c}\tilde{n}_c & \bar{g} \end{pmatrix} \quad (4)$$

where $\tilde{n}_i \equiv \bar{n}_i + 1$ with $\bar{n}_h = (e^{(E_a - E_1)/(k_B T_h)} - 1)^{-1}$ and $\bar{n}_c = (e^{(E_b - E_1)/(k_B T_c)} - 1)^{-1}$ (k_B is Boltzmann constant) representing the mean occupation of reservoir modes at energy $E_a - E_1$ and $E_b - E_1$, respectively, while $\bar{n}_l$ is the occupation of the cavity mode which is assumed to be held fixed at any desired value by manupulating external parameters, e.g., by changing the cavity volume,

reflectors, etc. The diagonal terms are

$$g_{11} = -\gamma_{1c}\bar{n}_c - \gamma_{1h}\bar{n}_h \quad (5)$$

$$g_{22} = -\gamma_{2c}\bar{n}_c - \gamma_{2h}\bar{n}_h \quad (6)$$

$$g_{aa} = -(\gamma_{1h} + \gamma_{2h})\tilde{n}_h - g^2\tilde{n}_l \quad (7)$$

$$g_{\beta\beta} = -(\gamma_{1c} + \gamma_{2c})\tilde{n}_c - g^2\bar{n}_l \quad (8)$$

$$\bar{g} = -\frac{1}{2}(\gamma_{1h} + \gamma_{2h})\bar{n}_h - \frac{1}{2}(\gamma_{1c} + \gamma_{2c})\bar{n}_c - \frac{1}{\tau_2} \quad (9)$$

$$g_{12} = \frac{1}{2}(\gamma_{12c}\bar{n}_c + \gamma_{12h}\bar{n}_h). \quad (10)$$

These rate-like equations are obtained with the help of standard approximations, namely large reservoirs whose state is only negligibly perturbed by the system, weak system-field coupling, the rotating wave approximation and a large and slowly varying density of states of near resonant field modes. (The latter approximation is known as the Weisskopf-Wigner approximation in Quantum optics, or the wide band approximation in condensed matter physics.) The derivation can be found in Ref. [9]. In appendix A we present a version of the derivation which has been modified to treat also the fluctuations of the QHE. These will be studied in section IV. The derivation in Ref. [9] essentially follows along the same lines as given in Appendix A with $\lambda = 0$.

In Eq. (4) the coherence is coupled to the populations via γ_{12c} and γ_{12h}. These coupling constants depend on the angle between transition dipoles. The maximal value of γ_{12h} is $\sqrt{\gamma_{1c}\gamma_{2c}}$ and the coupling vanishes when $\gamma_{12c} = 0$, with similar relations for γ_{12h}. We therefore view γ_{12c} and γ_{12h} as parameters which can control the value of the coherence ρ_{12} at steady state, albeit in a complicated manner. Only the real part ($\bar{\rho}_{12}$) of the coherence couples to the population dynamics for degenerate levels $|1\rangle, |2\rangle$.

Transitions between system states involve energy exchange with the different photon reservoirs. These can be assigned different thermodynamical interpretations based on the nature of the reservoirs. The two thermal reservoirs contain incoherent, fluctuating electromagnetic fields. Previous work have demonstrated that such photon reservoir behave like thermal baths [11]. Therefore energy taken from (or given to) such reservoirs should be interpreted as heat, and is accompanied by an appropriate change in the entropy of the reservoir. In contrast, transitions between the states $|a\rangle, |b\rangle$ are coupled to an athermal reservoir. We assume that all the energy involved in this transition can be utilized, and therefore interpret it as work. This means that even though the form of the transition rates connecting two populations in Eq. (4) is similar, the interpretation is different because of the different nature of the reservoir degrees of freedom (which were integrated out).

It should be stressed that we have kept the description of the $|a\rangle \leftrightarrow |b\rangle$ transition as one coupled to a field mode to keep the notations of Ref. [9]. This transition is not directly coupled to any coherence and therefore all the results presented below will apply to models with a different mechanism coupled to the $|a\rangle \leftrightarrow |b\rangle$ transition,

such as a charge transfer across a voltage difference, or a chemical catalysis. All that is needed is to replace the rates $\mathcal{L}_{ab}$, $\mathcal{L}_{ba}$ with thermodynamically consistent rates describing the process of interest (while modifying g_{aa}, g_{bb} accordingly).

The energy exchanged with different reservoirs are strongly coupled since, for instance, a cycle of transitions $a \to b \to 1, 2 \to a$ always involves an absorption of a photon from the hot reservoir, an emission of one photon into the cold reservoir and the cavity mode. This results in two possible steady-state scenarios [13]. The system can work either as a quantum heat engine (QHE) - it can extract energy from the hot bath T_h, perform some work on the radiation field and reject the unused energy to the cold bath T_c - or as a refrigerator which uses work to pump heat from the cold to the hot reservoirs.

III. QHE STEADY STATE

The steady state solution for the populations and the coherence is obtained by solving $\mathcal{L}\rho^s = 0$. In Fig. (2), we depict the variation of the steady state ρ^s with the temperature of the cold bath. The steady state heat current I_h between the hot reservoir and the system is

$$I_h = (E_a - E_1)g^2\left(\rho_{aa}^s \tilde{n}_l - \rho_{bb}^s \bar{n}_l\right). \qquad (11)$$

At steady state, Eq. (11) is proportional to the power of the QHE as defined in Ref. [9] (see Eq. (11) there). In the inset of Fig. (2) we plot (dotted curve) I_h as
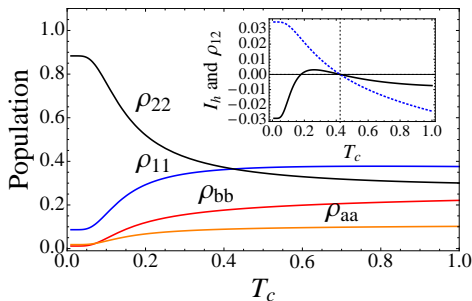

FIG. 2. (Color online) System state populations as function of the cold bath temperature for $T_h = g = n_l = \gamma_{1h} = 1.0$, $\gamma_{1c} = \gamma_{2h} = 0.1$ and $\gamma_{2c} = 2.0$. Inset shows the change in the coherence (solid curve) and the steady state current with T_c. Dotted vertical line at $T_c \approx .42$ indicates the temperature where the net current is zero (see the text).

function of T_c. It clearly manifests two regimes, heat engine ($I_h > 0$) and refrigerator ($I_h < 0$).

A general expression for the steady state heat current is given in appendix B, see Eqs. (B1) and (B2). In the following we show that in different parameter regimes coherence can either enhance or reduce the current.

First we note that for a symmetric coupling configuration, $\gamma_{1c} = \gamma_{2c} = \gamma_c$, $\gamma_{1h} = \gamma_{2h} = \gamma_h$, together

with maximal coherence couplings, $\gamma_{12c} = \sqrt{\gamma_{1c}\gamma_{2c}}$ and $\gamma_{12h} = \sqrt{\gamma_{1h}\gamma_{2h}}$, the effects of coherences vanish ($\rho_{12}^s = 0$) at steady state and the heat current is

$$I_h = \frac{2g^2\gamma_h\gamma_c[\tilde{n}_l\tilde{n}_c\bar{n}_h - \tilde{n}_h\bar{n}_l\bar{n}_c]}{\mathcal{D}(\gamma_h\bar{n}_h + \gamma_c\bar{n}_c)}(E_a - E_1) \qquad (12)$$

with $\mathcal{D} = [1 + 2\alpha_h][g^2\bar{n}_l - \gamma_h\bar{n}_h] + [1 + 2\alpha_c][g^2\tilde{n}_l + \gamma_h(2 + 3\bar{n}_h)]$, where we have used, $\alpha_c = \gamma_c(1 + \bar{n}_c)/(\gamma_h\bar{n}_h + \gamma_c\bar{n}_c)$ and similarly for α_h.

From the general expressions for the current, Eqs. (B1) and (B2), for $\gamma_{1h} = \gamma_{2h}$, $\gamma_{12h} = 0$ and $\bar{n}_l >> 1$, we can derive an approximate expression for the current

$$I_h = I_h^0\left[\frac{1 - \frac{f}{Q}}{1 - \frac{f(1 + 2\bar{n}_c)}{\alpha}}\right] \qquad (13)$$

where I_h^0 is the current in absence of coherences [see Eq. (B3)], $Q = (\alpha_{1c} + \alpha_{2c})/\tilde{n}_c$, $\alpha = 2 + \alpha_{1c} + \alpha_{2c} + \alpha_{1h} + \alpha_{2h}$, and $f = 2\gamma_{12c}^2\bar{n}_c/[\gamma_{1c}(\gamma_{2c}\bar{n}_c + \gamma_{2h}\bar{n}_h) + \gamma_{2c}(\gamma_{1c}\bar{n}_c + \gamma_{1h}\bar{n}_h)]$. Since $Q < \alpha/(1 + 2\bar{n}_c)$, we note that in this limit, the current is reduced by the coherences. Similar coherence dependence is found for $\gamma_{1h} = \gamma_{2h}$, $\gamma_{12c} = 0$ and $\bar{n}_l >> 1$. For $\bar{n}_l < 1$ with $\gamma_{1h} = \gamma_{2h}$, we find that current can be either enhanced or suppressed depending on the relative values of the induced coherences due to the hot and the cold baths. This is shown in the Fig. (3), which compares the value of the steady state current for finite γ_{12c} and γ_{12h} to its value for $\gamma_{12c} = \gamma_{12h} = 0$. Our results indicate that in order to enhance the QHE power using quantum coherences, the average occupation in the cavity mode must be kept less than the unity.
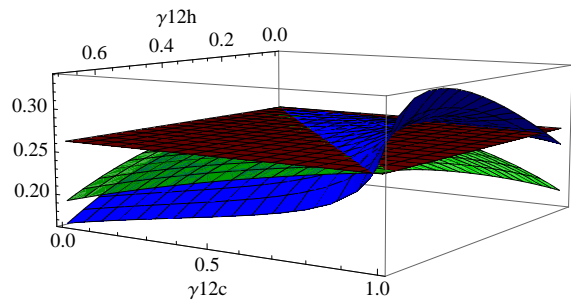

FIG. 3. (Color online) The steady state heat current as function of coherences induced by the hot and cold baths for $\gamma_{1h} = \gamma_{2h} = 0.7$, $T_c = 0.2$, $\gamma_{1c} = 0.5$, $\gamma_{2c} = 2.0$, $g = 100$, $E_a = 1.5$, $E_1 = E_2 = 0.1$, $E_b = 0.4$. The green and the blue surfaces represent variation in the current for $\bar{n}_l = 100$ and $\bar{n}_l = 0.01$, respectively. The red surface corresponds to the current without coherences [Eq. S-24] for $\bar{n}_l = .01$. The y-axis for the green surface ($\bar{n}_l = 100$) has been scaled such that the current without coherences for $\bar{n}_l = 100$ coincides with the red surface ($\bar{n}_l = .01$).

IV. FLUCTUATIONS

We now consider a measurement in which the QHE is brought to its steady state, and then the energy, or

equivalently the number of photons k, that it exchanges over a time t with one of the reservoirs - here chosen to be the hot reservoir - is mesaured. Due to the stochastic nature of the dynamics repetitions of the measurement will result in different values. By repeating the process many times one can calculate the probability distribution of the heat exchanged with the reservoir. We are interested to find out how does the coherence of the system affect this distribution.

To quantify the heat fluctuations at steady state we follow the measurement procedure outlined in [25]. The FCS of the heat exchange can be calculated using a twisted generator $\mathcal{L}(\lambda)$, where an auxiliary field λ is introduced in the transitions involving heat exchange with the reservoir of interest. For the heat exchanged with the hot reservoir the twisted generator $\mathcal{L}(\lambda)$ is

$$\mathcal{L}(\lambda) =$$
$$\begin{pmatrix} g_{11} & 0 & \gamma_{1h;\lambda}\tilde{n}_h & \gamma_{1c}\tilde{n}_c & -2g_{12} \\ 0 & g_{22} & \gamma_{2h;\lambda}\tilde{n}_h & \gamma_{2c}\tilde{n}_c & -2g_{12} \\ \gamma_{1h;-\lambda}\bar{n}_h & \gamma_{2h;-\lambda}\bar{n}_h & g_{aa} & \frac{g^2\bar{n}_l}{\gamma_l} & 2\gamma_{12h;-\lambda}\bar{n}_h \\ \gamma_{1c}\bar{n}_c & \gamma_{2c}\bar{n}_c & \frac{g^2\tilde{n}_l}{\gamma_l} & g_{\beta\beta} & 2\gamma_{12c}\bar{n}_c \\ -g_{12} & -g_{12} & \gamma_{12h;\lambda}\tilde{n}_h & \gamma_{12c}\tilde{n}_c & \bar{g} \end{pmatrix}$$
$$(14)$$

where, $\gamma_{X;\lambda} = \gamma_X e^{i\lambda}$. Equation (14) is derived from the Hamiltonian in appendix A. Note that the auxiliary field, λ, appears not only in the transition connecting populations, but also in transition between coherences and populations.

The probability distribution of the heat exchange can be calculated from Eq. (14) in a standard way by propagating the Lindblad equation with $\mathcal{L}(\lambda)$, tracing over populations, and then calculating an inverse Fourier transform with respect to λ, as explained in appendix C.

Probability distributions for the number of photons transferred are shown in Fig. (4) for the measurement time $t = 1000$ and temperatures spanning both the heat engine and the refrigerator regimes. Coherence clearly affects the distributions. In all cases, the central part of the distribution function can be approximated very well by a Gaussian. Coherence reduces thermal fluctuations in the heat current as is evident by the variance. This reduction is more pronounced when the system operates as a refrigerator (absorbing a coherent cavity photon and transferring heat from the cold to the hot bath), as shown in the inset of Fig. (4).

We now compare different distributions to their counterparts, calculated without coherence. In Fig. (5), we show the distributions for the heat engine regime (left panel), where we have centered all distributions around the mean transfer. The distribution is virtually unaffected by coherence. In the refrigerator regime (right panel), the distributions with and without coherence are clearly different.

The Fano parameter, $FP = \frac{\langle k^2 \rangle - \langle k \rangle^2}{\langle k \rangle}$, has been extensively used [28, 29] to quantify non-Poisson character of
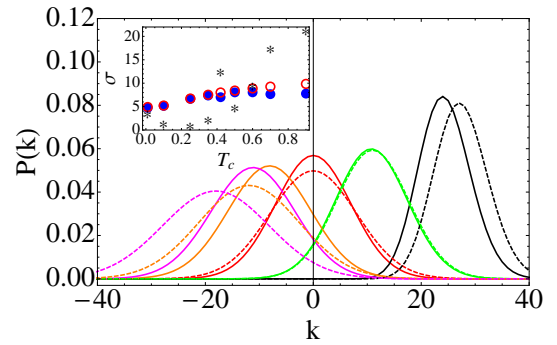

FIG. 4. (Color online) Probability distribution of the number of photons transferred between the hot bath and the system, k, for $t = 1000$, $T_c = 0.01$ (black), $T_c = 0.25$ (green), $T_c = 0.42$ (red), $T_c = 0.70$ (orange), and $T_c = 0.90$ (magenta) [T_c increasing from right to left]. Other parameters are the same as given in Fig. (2). Solid and dotted curves denote results for the maximum coherence $\gamma_{12h(c)} = \sqrt{\gamma_{1h(c)}\gamma_{2h(c)}}$ and no coherence $\gamma_{12h(c)} = 0$, respectively. For $T_c \geq .42$ the system operates as a refrigerator. Inset shows standard deviation (σ) at different temperatures with (filled circles) and without (empty circles) coherences. Stars represent the percentage change in σ due to coherences.
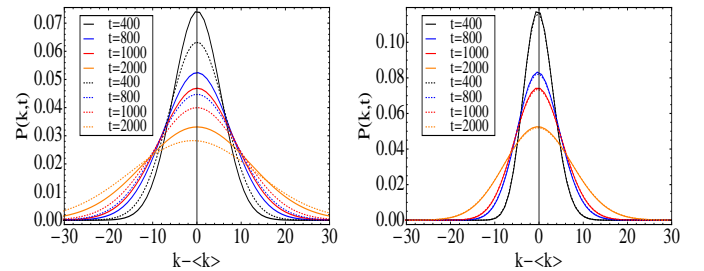

FIG. 5. (Color online) Probability distribution of the number of photons transferred for different measurement times (increasing from top to bottom) in the heat engine regime, $T_c = 0.12$ (left panel) and refrigerator regime $T_c = 0.95$ (right panel). Other parameters are the same as in Fig.(2). Solid and dotted curves have the same meaning as in Fig. (4).

the statistics ($FP = 0$ for Poisson statistics). In Fig. (6) we present this parameter over a range of T_c with and without coherences for small values of $.00001 < n_l < .02$. It shows a minimum at small T_c, but the statistics remains super-Poisson ($FP > 0$) over the whole range of T_c. For large values of n_l, the Fano parameter diverges (shown in the inset) at $T_c = \frac{E_b - E_1}{(E_a - E_1)/T_h - k_B \ln(1 + 1/\bar{n}_l)}$ where $\langle k \rangle = 0$. Coherence tends to decrease the super Poisson character of the statistics as the cold bath temperature is increased.

Interestingly, we find that even though coherences influence the full statistics, a coherence-independent steady state fluctuation relation still holds. This can be demonstrated by showing that $\mathcal{L}(\lambda)$ satisfies a simple identify

$$U^{-1}\mathcal{L}(\lambda)U = \mathcal{L}^T(-\lambda + i\alpha) \qquad (15)$$

where $U = \text{diag}\{r, r, r\frac{\bar{n}_c\bar{n}_l}{\tilde{n}_c\tilde{n}_l}, r\frac{\bar{n}_c}{\tilde{n}_c}, \frac{r}{2}\}$ for any r, and $\mathcal{L}^T$ is the transpose of $\mathcal{L}$. The parameter

$$\alpha = \ln\frac{\tilde{n}_h\bar{n}_c\bar{n}_l}{\tilde{n}_l\tilde{n}_c\bar{n}_h} = \frac{E_a - E_1}{k_B T_h} - \frac{E_b - E_1}{k_B T_c} + \ln\frac{\bar{n}_l}{\bar{n}_l + 1} \quad (16)$$

is an affinity which describes the effective thermodynamic force driving the system away from its equilibrium.
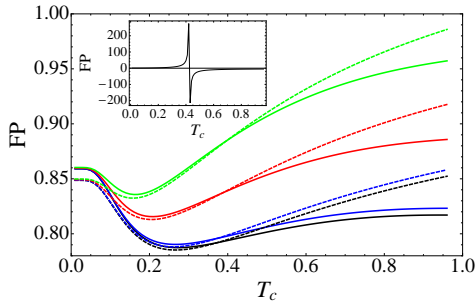

FIG. 6. Fano parameter for different values of $n_l = .0001, .001, .01, .02$ (increasing from bottom to top). Solid and dashed curves represent the results with and without the coherences, respectively. Inset ($n_l = 1.0$) shows the divergence of the Fano parameter at the point where the current vanishes.

The similarity transformation, Eq. (15), implies that $\mathcal{L}(\lambda)$ and $\mathcal{L}(-\lambda+i\alpha)$ have the same eigenvalues, resulting in the fluctuation relation,

$$\frac{P(k,t)}{P(-k,t)} = e^{\alpha k}. \quad (17)$$

Equation (17) holds asymptotically in the long observation time limit. It is clearly a steady-state quantum fluctuation relation, similar to those obtained by Jarzynski and Wójcik [30] and Andrieux *et. al.* [31]. (See Refs. [25, 26] for comprehensive reviews of quantum fluctuation relations.) One of the appealing properties of the QHE model studied here is that the fluctuation relation can be obtained from a rate-like equation in which quantum coherence plays an explicit role. Note that α depends only on the bath distribution functions (we assume that $\bar{n}_l$, the number of photons in the cavity mode, is held fixed). Therefore Eq. (17) is independent of the value of quantum coherence ($\gamma_{12c}, \gamma_{12h}$).

V. SUMMARY

To summarize, we have considered a model of a quantum heat engine which was previously studied as an example of a system whose thermodynamical properties are influenced by quantum coherence. We have obtained a closed expression for the steady state current and have found that for small cavity occupation the performance of the QHE can be enhanced by coherence.

We further considered the fluctuations around steady state of the QHE. The numerical results presented in

Figs. 4-6 clearly demonstrate that the distribution of exchanged heat depend on the coupling parameters that control the amount of coherence. An asymptotic fluctuation theorem for the fluctuations in the heat transferred between the hot bath and the QHE is derived analytically. Interestingly, our calculations show that a coherence independent fluctuation theorem, with an affinity that depends only on properties of the external reservoirs, holds.

Appendix A: Derivation of equations of motion for the reduced density matrix

In order to compute the full statistics of fluctuations, we follow the two-point measurement procedure as described in Ref. [25]. The generating function for k-quanta transfer between the hot reservoir and the system is obtained as

$$G(\lambda, t) = \text{Tr}_F\{\hat{\rho}_T(\lambda, t)\} \quad (A1)$$

where Tr_F is the full trace in the space of system + reservoirs + cavity, $\rho_T(\lambda = 0, t)$ is the density matrix of the total system. We make projections (measurements) in the hot reservoir and assume that the first measurement is performed at time $t = 0$, when the system-reservoirs coupling is turned on and the system density matrix is diagonal, i.e. initially ($t = 0$) the system is in pure quantum state. The second measurement is made after a time t. The time evolution of $\hat{\rho}_T(\lambda, t)$ is given by ($\hbar = 1$),

$$\hat{\rho}_T(\lambda, t) = e^{-i\hat{H}_T(\lambda)t}\hat{\rho}_T e^{i\hat{H}_T(-\lambda)t} \quad (A2)$$

where $H_T(\lambda) = \hat{H}_0 + \hat{V} + \hat{H}_c + \hat{H}_h(\lambda)$, with $\hat{H}_0$ and $\hat{H}_c$ given by the first and the second terms (where $k \in$ cold reservoir) on the rhs of Eq. (2), respectively, and

$$\hat{H}_h(\lambda) = e^{-i\lambda/2}\sum_{q,i=1,2} g_{iq}\hat{a}_q\hat{B}_{ai} + h.c. \quad (A3)$$

where $q \in$ hot reservoir. From (A2), we get,

$$\frac{\partial}{\partial t}\rho_T(\lambda, t) = -i[\hat{H}(\lambda)\rho_T(\lambda, t) - \rho_T(\lambda, t)\hat{H}(-\lambda)] \quad (A4)$$

Tracing over reservoirs and cavity modes, and defining $\hat{\rho}(\lambda, t) = \text{Tr}_R\{\rho_T(\lambda, t)\}$, we get

$$\frac{\partial}{\partial t}\hat{\rho}(\lambda, t) = -i\,\text{Tr}_R\{[\hat{H}(\lambda)\rho_T(\lambda, t) - \rho_T(\lambda, t)\hat{H}(-\lambda)]\} \quad \text{(A5)}$$

Up to second order in the coupling to the reservoirs and the cavity, and assuming the Markovian approximation, the right hand side gives,

$$\frac{\partial}{\partial t}\hat{\rho}(\lambda, t) = -i[\hat{H}_0, \hat{\rho}(\lambda, t)] - \Omega_{ph}\pi\sum_{i,i'}\left[g_{ih}g^*_{i'h}\left\{\hat{B}_{ai}\hat{B}^\dagger_{ai'}\hat{\rho}(\lambda, t)\tilde{n}_h(\omega_{ai'}) - \text{e}^{-i\lambda}\bar{n}_h(\omega_{ai'})\hat{B}_{ai}\hat{\rho}(\lambda, t)\hat{B}^\dagger_{ai'}\right.\right.$$

$$- \text{e}^{i\lambda}\tilde{n}_h(\omega_{ai'})\hat{B}^\dagger_{ai'}\hat{\rho}(\lambda, t)\hat{B}_{ai} + \bar{n}_h(\omega_{ai'})\hat{\rho}(\lambda, t)\hat{B}^\dagger_{ai'}\hat{B}_{ai}\right\} + g_{i'h}g^*_{ih}\left\{\tilde{n}_h(\omega_{ai'})\hat{\rho}(\lambda, t)\hat{B}_{ai'}\hat{B}^\dagger_{ai}\right.$$

$$- \text{e}^{-i\lambda}\bar{n}_h(\omega_{ai'})\hat{B}_{ai'}\hat{\rho}(\lambda, t)\hat{B}^\dagger_{ai} - \text{e}^{i\lambda}\tilde{n}_h(\omega_{ai'})\hat{B}^\dagger_{ai}\hat{\rho}(\lambda, t)\hat{B}_{ai'} + \bar{n}_h(\omega_{ai'})\hat{B}^\dagger_{ai}\hat{B}_{ai'}\hat{\rho}(\lambda, t)\right\}$$

$$+ g_{i'c}g^*_{ic}\left\{\tilde{n}_c(\omega_{bi'})\hat{\rho}(t)\hat{B}_{bi'}\hat{B}^\dagger_{bi} - \bar{n}_c(\omega_{bi'})\hat{B}_{bi'}\hat{\rho}(\lambda, t)\hat{B}^\dagger_{bi} - \tilde{n}_c(\omega_{bi'})\hat{B}^\dagger_{bi}\hat{\rho}(\lambda, t)\hat{B}_{bi'}\right.$$

$$+ \bar{n}_c(\omega_{bi'})\hat{B}^\dagger_{bi}\hat{B}_{bi'}\hat{\rho}(\lambda, t)\right\} + g_{ic}g^*_{i'c}\left\{\tilde{n}_c(\omega_{bi'})\hat{B}_{bi}\hat{B}^\dagger_{bi'}\hat{\rho}(t) - \bar{n}_c(\omega_{bi'})\hat{B}_{bi}\hat{\rho}(\lambda, t)\hat{B}^\dagger_{bi'} - \tilde{n}_c(\omega_{bi'})\hat{B}^\dagger_{bi'}\hat{\rho}(\lambda, t)\hat{B}_{bi}\right.$$

$$\left.\left.+ \bar{n}_c(\omega_{bi'})\hat{\rho}(\lambda, t)\hat{B}^\dagger_{bi'}\hat{B}_{bi}\right\}\right] - \pi|g_{bl}|^2\left[\tilde{n}_l(\omega_{ab})\hat{B}_{ab}\hat{B}^\dagger_{ab} - 2n_l(\omega_{ab})\hat{B}_{ab}\hat{\rho}(\lambda, t)\hat{B}^\dagger_{ab}\right.$$

$$\left.- 2\tilde{n}_l(\omega_{ab})\hat{B}^\dagger_{ab}\hat{\rho}(\lambda, t)\hat{B}_{ab} + \bar{n}_l(\omega_{ab})\hat{\rho}(\lambda, t)\hat{B}^\dagger_{ab}\hat{B}_{ab} + \tilde{n}_l(\omega_{ab})\hat{\rho}(\lambda, t)\hat{B}_{ab}\hat{B}^\dagger_{ab} + n_l(\omega_{ab})\hat{B}^\dagger_{ab}\hat{B}_{ab}\hat{\rho}(\lambda, t)\right] \quad \text{(A6)}$$

where we have indicated the couplings with the hot and the cold baths by subscript h and c, respectively, $\omega_{ij} = E_i - E_j$. The mode populations are $\bar{n}_x = \text{Tr}\{\hat{a}^\dagger_x\hat{a}_x\hat{\rho}_x\}$, where x corresponds to either hot ($x = h$), cold ($x = c$) reservoirs, or the cavity mode ($x = l$), and $\tilde{n}_x = 1 + \bar{n}_x$.

Ω_{ph} is the density of states of thermal reservoirs which is assumed to be independent of energy and identical for the two reservoirs.

Defining, $\rho_{ij} \equiv \langle i|\hat{\rho}|j\rangle$, we obtain the following set of coupled equations for the populations, ρ_{ii}, and the real part of the coherence $\bar{\rho}_{12}$.

$$\frac{\partial}{\partial t}\rho_{11} = -\left(\gamma_{1c}\bar{n}_c(\omega_{b1}) + \gamma_{1h}\bar{n}_h(\omega_{a1})\right)\rho_{11} + \text{e}^{i\lambda}\gamma_{1h}\tilde{n}_h(\omega_{a1})\rho_{aa} + \gamma_{1c}\tilde{n}_c(\omega_{b1})\rho_{bb}$$
$$- \left(\gamma_{12c}\bar{n}_c(\omega_{b2}) + \gamma_{12h}\bar{n}_h(\omega_{a2})\right)\bar{\rho}_{12} \quad \text{(A7)}$$

$$\frac{\partial}{\partial t}\rho_{22} = -\left(\gamma_{2c}\bar{n}_c(\omega_{b2}) + \gamma_{2h}\bar{n}_h(\omega_{a2})\right)\rho_{22} + \text{e}^{i\lambda}\gamma_{2h}\tilde{n}_h(\omega_{a2})\rho_{aa} + \gamma_{2c}\tilde{n}_c(\omega_{b2})\rho_{bb}$$
$$- \left(\gamma_{12c}\bar{n}_c(\omega_{b1}) + \gamma_{12h}\bar{n}_h(\omega_{a1})\right)\bar{\rho}_{12} \quad \text{(A8)}$$

$$\frac{\partial}{\partial t}\rho_{aa} = \gamma_{1h}\text{e}^{-i\lambda}\bar{n}_h(\omega_{a1})\rho_{11} + \gamma_{2h}\text{e}^{-i\lambda}\bar{n}_h(\omega_{a2})\rho_{22} - \left(\gamma_{1h}\tilde{n}_h(\omega_{a1}) + \gamma_{2h}\tilde{n}_h(\omega_{a2}) + g^2\tilde{n}_l(\omega_{ab})\right)\rho_{aa}$$
$$+ \gamma_{12h}\text{e}^{-i\lambda}\left(\bar{n}_h(\omega_{a1}) + \bar{n}_h(\omega_{a2})\right)\bar{\rho}_{12} + g^2\bar{n}_l(\omega_{ab})\rho_{bb} \quad \text{(A9)}$$

$$\frac{\partial}{\partial t}\rho_{bb} = \gamma_{1c}\bar{n}_c(\omega_{b1})\rho_{11} + \gamma_{2c}\bar{n}_c(\omega_{b2})\rho_{22} + g^2\bar{n}_l(\omega_{ab})\rho_{aa} + \gamma_{12c}\left(\bar{n}_c(\omega_{b1}) + \bar{n}_c(\omega_{b2})\right)\bar{\rho}_{12}$$
$$- \left(\gamma_{1c}\tilde{n}_c(\omega_{b1}) + \gamma_{2c}\tilde{n}_c(\omega_{b2}) + g^2\bar{n}_l(\omega_{ab})\right)\rho_{bb} \quad \text{(A10)}$$

and

$$\frac{\partial}{\partial t}\bar{\rho}_{12} = -\frac{1}{2}\left(\gamma_{12h}\bar{n}_h(\omega_{a1}) + \gamma_{12c}\bar{n}_c(\omega_{b1})\right)\rho_{11} - \frac{1}{2}\left(\gamma_{12h}\bar{n}_h(\omega_{a2}) + \gamma_{12c}\bar{n}_c(\omega_{b2})\right)\rho_{22}$$

$$+ \frac{1}{2}\gamma_{12h}e^{i\lambda}\left(\bar{n}_h(\omega_{a1}) + \bar{n}_h(\omega_{a2})\right)\rho_{aa} + \frac{1}{2}\gamma_{12h}\left(\bar{n}_c(\omega_{b1}) + \bar{n}_c(\omega_{b2})\right)\rho_{bb} - i\omega_{12}\bar{\rho}_{12}$$

$$- \frac{1}{2}\left(\gamma_{1h}\bar{n}_h(\omega_{a1}) + \gamma_{2h}\bar{n}_h(\omega_{a2}) + \gamma_{1c}\bar{n}_c(\omega_{b1}) + \gamma_{2c}\bar{n}_c(\omega_{b2})\right)\bar{\rho}_{12} \tag{A11}$$

where we have further defined the couplings,

$$\gamma_{1x} = \frac{\pi\Omega_{ph}}{2}|g_{1x}|^2, \gamma_{12x} = \frac{\pi\Omega_{ph}}{2}g_{1x}g_{2x}. \tag{A12}$$

For the degenerate case, $\omega_{a1} = \omega_{a2}$, $\omega_{b1} = \omega_{b2}$, we recover the results in Eq. (14).

Appendix B: Calculation of the steady-state current

At steady state, $\dot{\rho} = 0$ and substituting $\lambda = 0$, the above equations become a set of coupled linear equations in the populations and coherence. This set can be solved analytically to obtain the steady state density matrix. The steady state heat current between the system and the hot bath is given by Eq. (11). Substituting for steady state values of ρ_{aa} and ρ_{bb}, we obtain,

$$I_h = \frac{g^2\tilde{n}_l}{\bar{g}\mathcal{D}}(E_a - E_1)\left[\bar{g}[(\beta_{11} + \beta_{22})\{\Delta_h\alpha_{1c}g_{12} + \gamma_{2h}\gamma_{12c}\bar{n}_h\tilde{n}_c\} - (2\gamma_{12h}\bar{n}_h + \Delta_h\beta_{11})\{g_{12}(\alpha_{1c} + \alpha_{2c}) - \gamma_{12c}\tilde{n}_c\}]\right.$$

$$\left. - \bar{g}^2\bar{n}_h(\gamma_{1h}\alpha_{1c} + \gamma_{2h}\alpha_{2c})\right] + \frac{g^2\bar{n}_l}{\bar{g}\mathcal{D}}(E_a - E_1)\left[\bar{g}[(\beta_{11} + \beta_{22})\{g_{12}(\Delta_h\alpha_{1h} - \tilde{n}_h(\gamma_{1h} + \gamma_{2h})) + \gamma_{2h}\gamma_{12h}\bar{n}_h\tilde{n}_h\}\right.$$

$$\left. - (2\gamma_{12h}\bar{n}_h + \Delta_h\beta_{11})\{g_{12}(\alpha_{1h} + \alpha_{2h}) - \gamma_{12h}\tilde{n}_h\}] + \bar{g}^2\bar{n}_c(\gamma_{1c}\alpha_{1h} + \gamma_{2c}\alpha_{2h})\right] \tag{B1}$$

where $\beta_{ii} = -(\gamma_{12h}\bar{n}_h + \gamma_{12c}\bar{n}_c)/(\gamma_{ih}\bar{n}_h + \gamma_{ic}\bar{n}_c), i = 1, 2$, $\Delta_h = \bar{n}_h(\gamma_{1h} - \gamma_{2h})$, and $\alpha_{ic} = \gamma_{ic}\tilde{n}_c/(\gamma_{ih}\bar{n}_h + \gamma_{ic}\bar{n}_c)$. The function $\mathcal{D}$ is

$$\mathcal{D} = (1 + \alpha_{1h} + \alpha_{2h})[(2\gamma_{12h}\bar{n}_h + \Delta_h\beta_{11})(g_{12} + \gamma_{12c}\tilde{n}_c) + \bar{g}(\gamma_{2h}\bar{n}_h - g^2\bar{n}_l - \Delta_h\alpha_{1c})]$$

$$- (1 + \alpha_{1c} + \alpha_{2c})[(2\gamma_{12h}\bar{n}_h + \Delta_h\beta_{11})(g_{12} + \gamma_{12h}\tilde{n}_h) + \bar{g}(\gamma_{2h}\bar{n}_h - g_{aa} - \Delta_h\alpha_{1h})]$$

$$+ (\beta_{11} + \beta_{22})[(\gamma_{2h}\bar{n}_h - g_{aa} - \Delta_h\alpha_{1h})(g_{12} + \gamma_{12c}\tilde{n}_c) - (\gamma_{2h}\bar{n}_h - g^2\bar{n}_l - \Delta_h\alpha_{1c})(g_{12} + \gamma_{12h}\tilde{n}_h)]. \tag{B2}$$

In the absence of coherences, i.e., $\gamma_{12c} = \gamma_{12h} = 0$, but for arbitrary couplings γ_{ix} where $i = 1, 2$ and $x = h, c$, the current is given by

$$I_h^0 = \frac{g^2(E_a - E_1)\left[\tilde{n}_l\bar{n}_h(\gamma_{1h}\alpha_{1c} + \gamma_{2h}\alpha_{2c}) - \bar{n}_l\bar{n}_c(\gamma_{1c}\alpha_{1h} + \gamma_{2c}\alpha_{2h})\right]}{(1 + \alpha_{1c} + \alpha_{2c})(g^2\tilde{n}_l + \gamma_{2h}(1 + 2\bar{n}_h) + \alpha_{1h}(\gamma_{1c}\bar{n}_c + \gamma_{2h}\bar{n}_h)) + (1 + \alpha_{1h} + \alpha_{2h})(g^2\bar{n}_l - \gamma_{2h}\bar{n}_h + \Delta_h\alpha_{1c})} \tag{B3}$$

where $\alpha_{1c(2c)} = \gamma_{1c(2c)}(1 + \bar{n}_c)/[\gamma_{1c(2c)}\bar{n}_c + \gamma_{1h(2h)}\bar{n}_h]$, similarly for $\alpha_{1h(2h)}$, and $\Delta_{h(c)} = [\gamma_{1h(1c)} - \gamma_{2h(2c)}]\bar{n}_{h(c)}$.

Appendix C: Cumulant generating function

The generating function (GF) corresponding to the probability of transferring k photons between the hot bath and the quantum engine is defined as

$$G(\lambda, t) \equiv \sum_k e^{i\lambda k}P(k, t). \tag{C1}$$

The number of transferred photons is proportional to the heat exchange. This generating function can be calcu-

lated using standard techniques,

$$G(\lambda, t) = \text{Tr}\,\rho(\lambda, t), \qquad \dot{\rho}(\lambda, t) = \mathcal{L}(\lambda)\rho(\lambda, t) \tag{C2}$$

where $\rho(\lambda, t = 0) = \rho^s$ and Tr denotes a sum over the populations.

We look for the fluctuations in the net photon transfer between the hot reservoir and the system. In this setup the hot reservoir serves as a "classical" detector. The moment generating function then allows us to compute the full steady state distribution function for the net number k photons transferred between the reservoir and the

QHE,

$$P(k,t) = \int \frac{d\lambda}{2\pi} e^{-i\lambda k} G(\lambda, t). \qquad (C3)$$

Equation (C3) immediately provides the heat distribution function, $P(h,t)$, for the transferred heat, $h = (E_a - E_1)k$, between the system and the hot bath during a binning time t.

One can also defined a cumulant generating function $S(\lambda)$ via $G(\lambda,t) = e^{tS(\lambda)}$. For long observation times, the cumulant generating function $S(\lambda)$ is dominated by

the eigenvalue of the generator $\mathcal{L}(\lambda)$ with the largest real part. In this limit only the dominant eigenvalue of $\mathcal{L}(\lambda)$ is required to calculate the full distribution function. The numerical results presented in the manuscript are based on a diagonalization of the twisted propagator $\mathcal{L}(\lambda)$. Finally, when the generating function is asymptotically dominated by the eigenvalue with the largest real part, it satisfies a symmetry relation, $G(\lambda) = G(-\lambda + i\alpha)$ which leads to the fluctuation relation when combined with Eq. (C3).

[1] A. L. Hammond, Science **178**, 732 (1972).
[2] A. Shah, P. Torres, R. Tscharner, N. Wyrsch, and H. Keppner, Science **285**, 692 (1999).
[3] See the special issue of Chemical Reviews **110**, (11) 6443-6936 (2010).
[4] B. J. Sambur, T. Novet and B. A. Parkinson, Science **330**, 63 (2010).
[5] B. Cho, W. K. Peters, R. J. Hill, T. L. Courtney, and D. M. Jonas, Nano Lett. **10**, 2498 (2010).
[6] R. D. Schaller and V. I. Klimnov, Phys. Rev. Lett. **92**, 186601 (2004).
[7] R. Baer and E. Rabani, Nano. Lett. **10**, 3277 (2010).
[8] R. Baer and E. Rabani, Chem. Phys. Lett. **227**, 496 (2010).
[9] M. O. Scully, K. R. Chapinb, K. E. Dorfmana, M. B. Kimb and A. Svidzinskya, PNAS **108**, 15097 (2011).
[10] M. O. Scully, Phys. Rev. Lett. **104**, 207701 (2010).
[11] H. E. D. Scovil and E. O. Schulz-DuBois, Phys. Rev. Lett., **2** , 262 (1959).
[12] E. Geva and R. Kosloff, Phys. Rev. E, **49**, 3903 (1994).
[13] E. Boukobza and D. J. Tannor, Phys. Rev. Lett. **98**, 240601 (2007).
[14] W. Shockley and H. J. Queisser, J. Appl. Phys. **32**, 510 (1961).
[15] S.Ya. Kilin, K. T. Kapale, and M. O. Scully, Phys. Rev. Lett. **100**, 173609 (2008).
[16] M. O. Scully, M. S. Zubairy, G. S. Agarwal and H. Walther, Science **299**, 862 (2003).
[17] T. Fujisawa, T. Hayashi, R. Tomita, and Y. Hirayama1, Science **312**, 1634 (2006).
[18] C. Flindta, C. Fricke, F. Hohls, T. Novotny, K. Netocny, T. Brandes, and R. J. Haug, PNAS **106**, 10116 (2009).
[19] Y.V. Nazarov and Ya.M. Blanter, Quantum Transport: Introduction to Nanoscience (Cambridge University Press, Cambridge, England, 2009).
[20] L. S. Levitov and G. B. Lesovik, JETP Lett. **58**, 230 (1993).
L. S. Levitov and M. Reznikov, Phys. Rev. B **70**, 115305 (2004).
S. Gustavsson, R. Leturcq, B. Simovic, R. Schleser, T. Ihn, P. Studerus, K. Ensslin, D. C. Driscol, and A. C. Gossard, Phys. Rev. Lett. **96**, 076605 (2006).
[21] D. J. Evans, E. G. D. Cohen, and G. P. Morriss, Phys. Rev. Lett., **71** , 2401 (1993).
[22] G. Gallavotti and E. G. D. Cohen, Phys. Rev. Lett., **74** , 2694 (1995).
[23] C. Jarzynski, Phys. Rev. Lett. **78**, 2690 (1997).
[24] G. E. Crooks, J. Stat. Phys. **90**, 1481 (1998); Phys. Rev. E **60**, 2721 (1999).
[25] M. Esposito, U. Harbola and S. Mukamel, Rev. Mod. Phys. **81**, 1665 (2009); Phys. Rev. B **75**, 155316 (2007);
[26] M. Campisi, P. Hänggi, and P. Talkner, Rev. Mod. Phys. **83**, 771 (2011).
[27] S. Mukamel, Phys. Rev. Lett. **90**, 170604 (2003).
[28] W. D. Oliver, J. Kim, R. C. Liu, and Y. Yamamoto, Science **284**, 299 (1999)
[29] K. Matsuo, M. C. Teich, and B. A. A. Saleh, Appl. Opt. **22**, 1898 (1983).
[30] C. Jarzynski and D. K. Wójcik, Phys. Rev. Lett., **92**, 230602 (2004).
[31] D. Andrieux, P. Gaspard, T. Monnai and S. Tasaki, New J Phys., **11**, 043014 (2009).